Thermochimica Acta, 106 (1986) 9–25
Elsevier Science Publishers B.V., Amsterdam – Printed in The Netherlands

MECHANISM OF ZINC SULPHIDE OXIDATION

R. DIMITROV *
Department of Chemical Technology, P. Hilendarsky University, 4000 Plovdiv (Bulgaria)

I. BONEV
Institute for Geology, Bulgarian Academy of Sciences, 1000 Sofia (Bulgaria)
(Received 22 January 1986)

ABSTRACT

Investigations have been carried out on the thermodynamics, kinetics and mechanism of oxidation of ZnS. The following methods were used: thermodynamic, DT, TG, chemical, phase chemical, gaseous and X-ray (structural, phase, micro-) analyses, scanning electronic microscopy, stereomicroscopy, electronography, analysis of kinetic data, etc.

Chemical potential diagrams (log P_{SO_2}–log P_{O_2}) have been constructed at various temperatures and the regions of stability of the separate compounds were defined.

A multi-strata, strongly porous, finely grained oxide product has been obtained. The layers have a thickness of 5–20 μm and are marked off by cracks up to 1–2 μm wide. This determines the evolution of the oxidation process of particles of the floatation concentrate in a fluidized bed at the high temperature of roasting zinc concentrates under a kinetic regime.

A mechanism is suggested for oxidation of a separate particle of ZnS, reporting both the evolution of the chemical process itself and the evolution of heat, heat and mass changes, and changes in the structure and porosity of the solid reagent and product.

Structural models are suggested in oxidizing lamellae and spherical particles of ZnS.

INTRODUCTION

The thermodynamics, kinetics, chemistry and mechanism of ZnS oxidation have been studied by a great number of investigators [1–36], but the results obtained differ considerably regarding the activation energy, oxidation regime, primary products, suggested reaction mechanism, etc. [30]. Sulphide behaviour is explained from the point of view of oxide [35,15], sulphate [34], adsorption and dissociation [33] theory, dissociation hypothesis [21], etc.

It can be seen that in the previous investigations the structure and purity of the sample, as well as the reaction conditions, are not described suffi-

* To whom correspondence should be addressed.

0040-6031/86/$03.50

ciently in most cases. The real structure and porosity of the product obtained, the specific surface, the spatial distribution of the pores regarding size and quantity on the solid reagent and the solid product obtained, the presence of donor and acceptor impurities and so on, have not been paid enough attention. The microscopic investigation of inclusions of oxide specimens in resins, as a basic method, does not give sufficient information about these important features.

Haufe [37] and Vanjukov and Zaitsev [35] suggest that the most objective information on the chemistry of solid sulphide oxidation could be obtained on the grounds of the general theory of the solid state. Substantial participation of Me^{2+}, S^{2-} and O^{2-} diffusion through the solid oxide product in the general process of oxidation is supposed to take place analogously to metal oxidation.

The chemistry and mechanism of ZnS oxidation are discussed in the literature [22,23,25,28,35,36]. Meanwhile, technical progress requires automatic control of heating processes. Rational designing and optimum control of roasters nowadays may be based only on actual knowledge of the mechanism of the processes of oxidation taking place.

EXPERIMENTAL

For years we have been carrying out systematic complex studies on metal sulphide oxidations, particularly ZnS [8,11,12,15,17,26,27,29–32,36].

The following methods have been used: thermodynamic, DT, TG, chemical, phase chemical, gaseous and X-ray (structural, phase, micro-) analyses, scanning electronic microscopy and stereomicroscopy, electronography, kinetic data analysis, etc.

The experiments were organized so that the possibility of secondary reactions taking place was a minimum, the influence of the diffusion factor was decreased and isothermal, or conditions close to these were created [37].

THERMODYNAMICS OF ZnS OXIDATION

On the grounds of contemporary thermodynamic data, using Tiomkin and Schwarzman's [29] method, thermodynamic analysis of 17 reactions from the system Zn–S–O was performed during roasting of zinc, copper–zinc and pyrite concentrates. The diagrams of the chemical potentials log P_{SO_2}–log P_{O_2} (Kellogg diagrams) for temperatures characteristic of the above process are drawn along with the relations $\Delta G_T^0 = f(T)$ and $\log K_p = f(T)$ (Fig. 1).

The equilibrium between Zn, ZnO, ZnS, $ZnO \cdot 2ZnSO_4$, $ZnSO_4$ and the gas phase, containing SO_2 and O_2, is reported. A polythermal spatial diagram for the region of $ZnO \cdot 2ZnSO_4$ stability is also drawn.

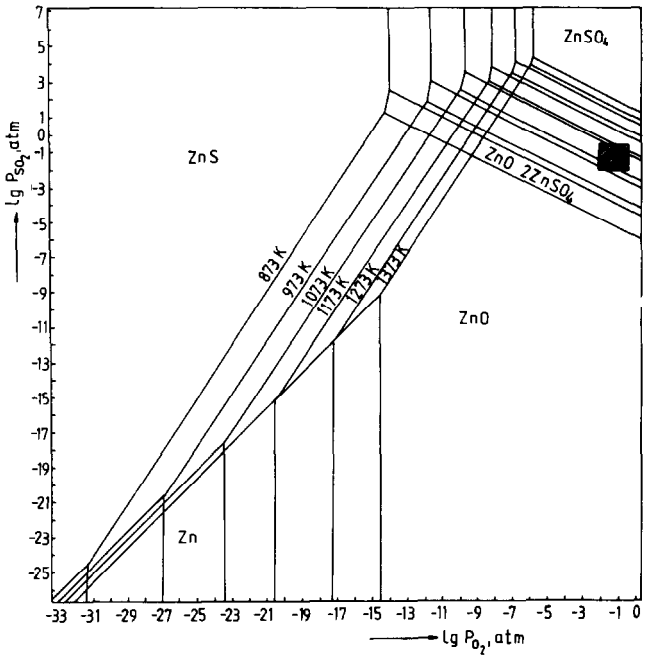

Fig. 1. Isothermal sections of the diagrams of the chemical potentials in the system Zn–S–O. The real gas phase contents at different points of the fluid bed during roasting of zinc concentrates are denoted by hatched squares.

Our industrial investigations, carried out in a roaster of a zinc plant, show that the fluid bed temperature along the height of the bed and the diameter of the furnace varies between certain limits (1073–1273 K). The SO_2 content of the gas mixture changes from 0–1% to 17% and that of oxygen from ~ 21% to ~ 1%.

The following points were established on the grounds of the thermodynamic analysis of the system Zn–S–O:

(1) the following consecutively stable phases of the process may be pointed out during oxidation at the roasting reactor conditions:

873 K: $ZnS–ZnO–ZnO \cdot 2ZnSO_4–ZnSO_4$
973 K: $ZnS–ZnO–ZnO \cdot 2ZnSO_4–ZnSO_4$
1073 K: $ZnS–ZnO–ZnO \cdot 2ZnSO_4–(ZnSO_4)$
1173 K: $ZnS–ZnO–(ZnO \cdot 2ZnSO_4)$
1223 K: ZnS–ZnO
1273 K: ZnS–ZnO

(The parentheses indicate that the phase is stable only at certain contents of the gaseous phase in the furnace.)

(2) ZnO is the primary product of ZnS oxidation for the roasting furnace conditions;

(3) zinc metal is stable at comparatively low partial pressures of O_2 and SO_2 in the gas phase (such conditions do not exist in the furnace);

(4) $ZnSO_4$ is stable at high P_{SO_2} values, which do not exist in this case; it is also stable at comparatively lower temperatures (for example 873, 973 K);

(5) compared to $ZnSO_4$, $ZnO \cdot 2ZnSO_4$ is stable at comparatively lower values of P_{SO_2} and P_{O_2} and its occurrence at lower temperatures of the process may be expected (973, 1073 and at given conditions, at 1173 K);

(6) on the grounds of Gibbs energy values, ΔG_T^0, oxidation should be expected to occur in the temperature range 973–1273 K, accompanied by the formation of, predominantly, $ZnO \cdot 2ZnSO_4$.

ZnS oxidation is a complex heterophase physicochemical process, the mechanism of which depends on the conditions of its performance. ZnO is expected to appear in the calcine from roasting zinc concentrates in a fluid bed, while the zinc sulphates, $ZnSO_4$ and $ZnO \cdot 2ZnSO_4$ may be expected to be present in the calcine from roasting copper–zinc and copper concentrates. The latter sulphates may occur at places of lower temperatures: in dust from the electrostatic precipitator, scales from the furnace hearth and the forechamber, as well as at the cooling elements in the bed during the roasting of zinc concentrates.

KINETICS OF ZnS OXIDATION

The kinetic investigations were conducted [15] on an original installation for DTA in a fluid bed [32].

The applicability of the equations, recommended by Levenspiel [39], Habashi [40] and Sohn and Goel [22], was checked for kinetic data processing in the system $S_1 + G_1 \rightarrow S_2 + G_2$:

(a) $1 - (1 - \alpha)^{1/F} = k\tau$

for porous products when the chemical reaction at the reagent–product interface is the limiting stage of the heterogeneous process;

(b) $1 - 2/3\alpha - (1 - \alpha)^{2/3} = k\tau$

TABLE 1

Activation energy in the oxidation of ZnS, sphalerite and marmatite in a fluid bed

Sulphide, mineral	Temperature interval (K)	Degree of completion of the process	E_a	
			kJ mol^{-1}	kcal mol^{-1}
ZnS amorphous	773–1073	0.01 –0.983	63.1	15.1
ZnS cubic	898–1173	0.007–0.996	111.6	26.7
ZnS hexagonal	883–1023	0.013–0.860	104.0	24.9
	1043–1243	0.048–0.993	84.0	20.1
Sphalerite	923–1173	0.01 –0.980	161.4	38.6
Marmatite	923–1173	0.02 –0.975	118.3	28.3

Crank–Ginstling–Brounshtein equation when the diffusion of the gaseous reagent through the product towards the unreacted core is the limiting stage.

$F = 3$ [22] for spherical particles, α is the degree of transformation, k is the rate constant, and τ is the time.

Our kinetic data linearize almost completely using the first equation. The calculated values of the apparent activation energies are given in Table 1 [30].

The calculated values of the activation energies for the five initial substances show (Habaschi [40], pp. 66–67) that the process takes place in a kinetically controlled regime ($E_a > 10$ kcal mol^{-1}). This is a logical result, bearing in mind that the process is carried out in a fluid bed, the size of the particles (0.16×10^{-3}–0.125×10^{-3} m), the great porosity and the complex structure of the oxide product obtained [26].

CHEMISTRY OF ZnS OXIDATION

Lamellae of synthetic hexagonal ZnS were oxidized at different temperatures and durations. The following phases were found on the surface by the electronographic method:

(a) ZnS, ZnO, $ZnSO_4$ and Zn at 800 K and 120, 600 and 1200 s;

(b) ZnS, ZnO, $ZnSO_4$ at 853 K (240 and 1200 s), 900 K (240, 480 and 720 s), 953 K (120, 240 and 480 s), 1048 K (60 and 300 s);

(c) ZnO, $ZnSO_4$ at 1048 K (600 s);

(d) ZnO at 1123 K (30 and 60 s), 1173 K (120 s), 1273 K (120 s).

The product, obtained on the surface of the lamella, is identified by X-ray phase analysis as ZnO.

Small particles (-0.16×10^{-3} and 0.125×10^{-3} m) of hexagonal ZnS [15] are oxidized in the fluid bed at conditions close to isothermal. The product obtained is subjected to X-ray phase analysis and chemical analysis. No sulphate was found by X-ray graphical analysis, or in a small sample of powder, oxidized in a stationary layer in the stream of air at 873 K for 5 h, using the same method.

The chemical phase analysis of particles, oxidized in the fluid bed at different conditions ($T = 913$–1173 K; $\tau = 10$–1200 s), shows a minimum quantity of zinc, bound as sulphate ($< 0.8\%$ zinc).

The recovery of large quantities of ZnO and small quantities of sulphate is logical, bearing in mind the conditions of the laboratory experiments. Aiming to obtain isothermal conditions, fluid bed roasting is conducted with samples of small weight (1×10^{-5} kg) and a large quantity of inert diluting agent. At the same time the product gas is continuously evacuated from the system. Under these conditions P_{SO_2} is insignificant and from the thermodynamic point of view the formation of ZnO is to be expected. According to Sohn and Goel [22], for kinetic reasons, the amount of sulphate in the

roasted product is usually small, even in cases where thermodynamic conditions for sulphate formation prevail.

The larger quantities of sulphate established by Frentz [34] are due to the experimental conditions: in a boat with a comparatively large quantity of sample [30].

The results of our derivatographic investigations [41] show that on polythermal oxidation of synthetic crystal ZnS, sphalerite and zinc concentrates, containing comparatively little iron (2.70%), no endo effects, characteristic of $ZnO \cdot 2ZnSO_4$ and $ZnSO_4$ dissociation, were observed. Such effects were noticed during oxidation of marmatite and high-iron concentrates (8.45%). This may be explained by the catalytic role of iron oxides in SO_2 to SO_3 oxidation. The increased partial pressure of SO_3 in different places determines the higher degree of sulphation.

The results of the chemical phase analysis of samples taken from the hearth and from the walls of the forechamber show the formation of substantial quantities of sulphates ($Zn_{sulphate} = 20–30\%$ [38]).

Conclusions from the thermodynamic analysis are confirmed experimentally.

The X-ray microanalysis of samples of hexagonal synthetic ZnS, oxidized under different conditions ($T = 873$, 1073 and 1273 K; $\tau = 0.5$ and 1 h),

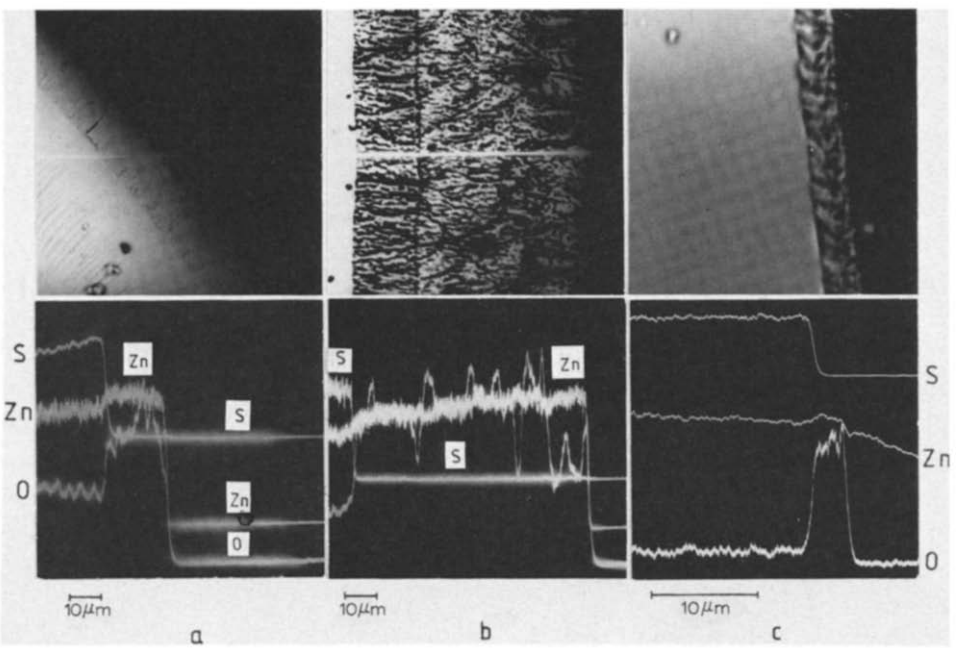

Fig. 2. Results from X-ray microanalysis along the line for Zn, S and O in a ZnS lamella, oxidized at different temperatures: (a) 873 K, 2 h, ×1000; (b) 973 K, 2 h, ×1000; (c) 1223 K, core (Fig. 3), ×3000.

show complete absence of sulphur in the oxidation product. Different apparatuses were used: SEMQ-ARL and JEOL Super Probe 733. Some of the results obtained are represented in Fig. 2. The X-ray microanalysis of areas shows that there is only one product. The X-ray phase analysis shows only ZnO. This does not exclude the eventual formation of unstable intermediate sulphate complexes [33] which, under the experimental conditions (large amount of excess air and rapid removal SO_2 from the reaction zone), immediately pass to the oxide phase.

MECHANISM OF ZnS OXIDATION

The experiments were carried out with microcrystal, synthetic, colourless, transparent ZnS of semiconductor purity, a rhombohedral 12R modification, obtained by crystallization from the gas phase. Lamellae (0.5×10^{-3}–1×10^{-3} m thick and 3–5×10^{-3} m wide and long) were used, cut at their splittable planes [(1010) and (0001)]. Separate grains, produced by arbitrary crushing and grinding of such materials, are formed namely from the thickest and most unreactive planes.

Experiments were also carried out with natural cubic sphalerites of low ($< 0.5\%$) and higher ($\sim 9\%$) iron contents.

Small pieces of ZnS were oxidized in an air stream under different conditions (temperature, time, O_2 content). The quantity of SO_2 given off in the process was determined iodometrically. The structure of samples, partially or completely oxidized, was studied along the cross sections, passing through their centres. Naturally, the split and gilded surface was observed directly by a scanning electron microscope with a microanalyser (JEOL Super Probe 733).

A completely oxidized sample consists of an oxide crust and an unoxidized central sulphide core (Figs. 3 and 4). The oxidized product replaces the sulphide samples pseudomorphically, entirely preserving its initial form (Fig. 3).

The oxide crust represents a fine-grained porous aggregate of ZnS of multi-layer structure and high porosity (Figs. 3 and 5). The thickness of the layers is 5–20 μm. They are arranged approximately parallel to the initial outer surface of the replaced sample and are differentiated clearly by layer cracks of up to 1–2 μm width.

The oxide layer is composed of isometric irregular grains of 0.1–0.5 μm diameter. A number of pores are observed between them, which occupy 3–5% of the overall area (Fig. 6). It was established that the cross sectional porosity was of anisotropic character. The pores, which have isometric or elongated forms, join together to form a system of elongated irregular channels directed towards the interior of the sample. They also join the

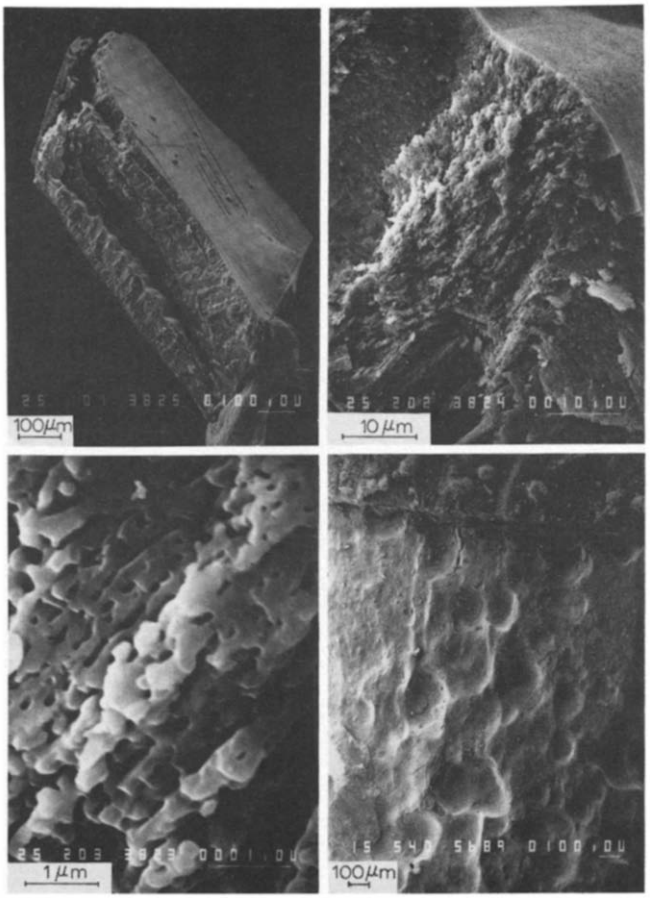

Fig. 3. Structure of the oxide coating of a ZnS lamella, oxidized at 1223 K for 1 h; linear scale in μm.

interlayer cracks. The number, dimensions and arrangement of the pores in the separate oxide layers deep in the particle are quite similar.

The total volume porosity of the oxide aggregate is rather high. It amounts to 36–38% by picnometric determination.

The theoretically calculated values, taking into consideration the molar volumes of the initial reagent, ZnS (23.83×10^{-6} m^3), and the product, ZnO (14.34×10^{-6} m^3), preserving the starting volume, is 39.8 vol.%.

The central unreacted sulphide core has a form similar to the initial sample, but the top and edges are rounded. Under observation at high magnification it turned out that the surface of the sulphide core is also coated with a thin porous layer. Actually, this is the initial stage of core oxidation with the formation of the next oxide layer occurring before its separation from the base (ZnS).

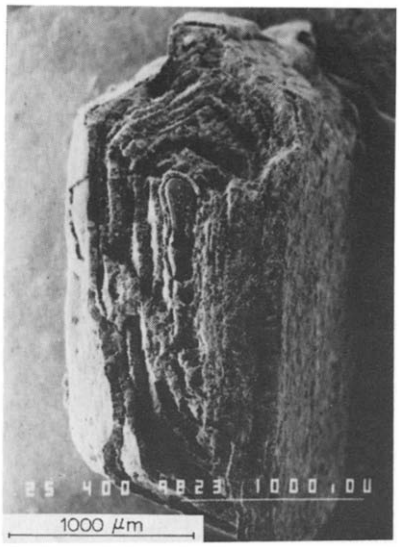

Fig. 4. Structure of the oxide coating of a ZnS lamella, oxidized at 1223 K for 40 min.

The profile microdrill analyses along the cross section (a flat parallel lamella, transversely cut from the core) show (Fig. 2) opposite changes of S and O contents at almost constant Zn content (a small relative increase in the oxide layer). The effect of radiation from the parallel Zn $L\beta$ on O $K\alpha$ (STE crystal analyser) was eliminated by differential energy discrimination.

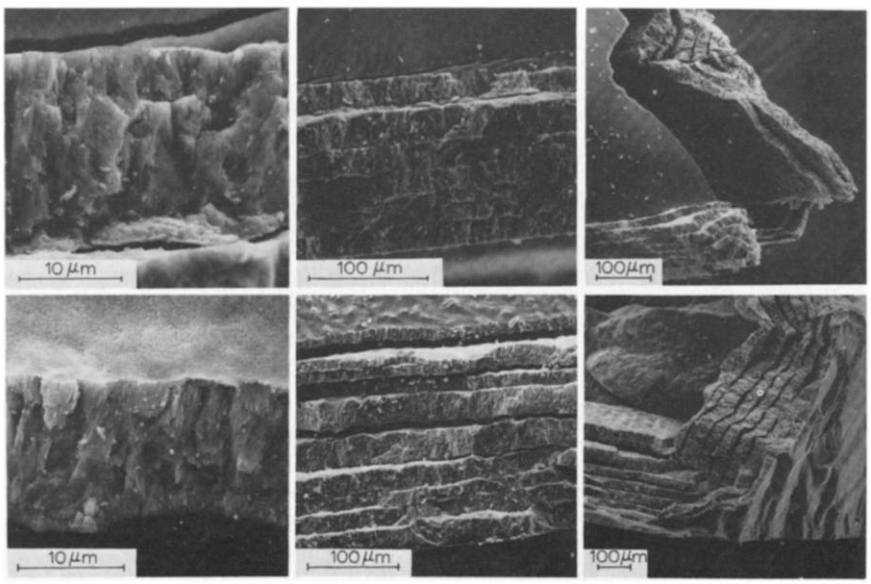

Fig. 5. Structure of the oxide coating of a ZnS lamella, oxidized at 1073 K for 0.5 and 1 h, SEM.

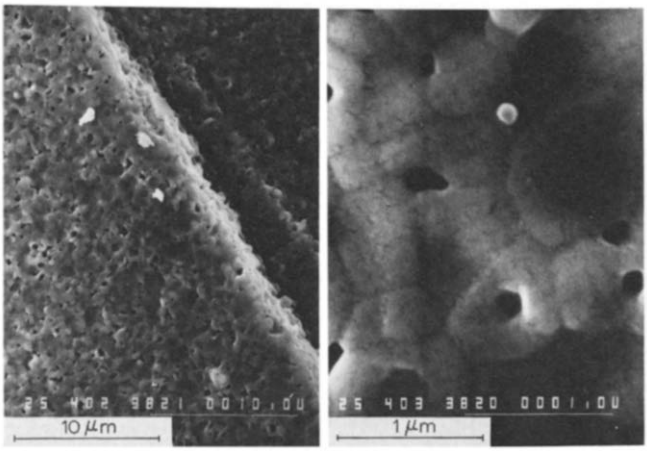

Fig. 6. Structure of the surface of a ZnS lamella, oxidized at 1073 K for 1 h, SEM; linear scale in μm.

The process of oxidation begins with the formation of oxide phase cores, ZnO, at multiple active points [15] from the sulphide surface. Cores of the subsequent polycrystal oxide layer continue to grow entirely in the sulphide mass on account of zinc atoms and oxygen entering from outside. The substantial porosity of the product ensures an oxygen supply to the reaction zone and removal of the SO_2 formed. The reaction is of topochemical and reconstructional character. Due to the similar growth rates of the oxide grains, the replacement front begins smoothly. The front acquires a wavy character on departure from the outer initial planes of the oxidized lamella. This is observed both on the inner oxide layers (Fig. 3) and on the unreacted sulphide core lying in front of them.

The substantial volumetric change during the reaction leads to the creation of tensile strains in the region of the oxide–sulphide interface. The periodic formation of concentric cracks, separating the consecutive oxide layers, may be explained by their growth up to a certain critical value. The moment of splitting of the oxide layer from the sulphide core is shown in Fig. 5. The formation and growth of the following oxide layer start with the uncovering of a fresh sulphide surface.

The kinetic curves, obtained by gas analysis (Fig. 7) show a periodic change (increased rate of SO_2 liberation). The number of impulses of the velocity curve exactly correlates with the number of oxide layers in the product. This testifies to the periodic uncovering of new reaction surfaces and intensification of the process at the onset of each oxidation cycle. The gradual increase in the overall course of the curve of SO_2 liberation reflects the gradual decrease of reaction surface in the depth of the oxidized particle.

Needle- and strip-like crystals of ZnS (Fig. 3), grown on the isometric oxide grains, were noticed at places on the surface of the inner concentric

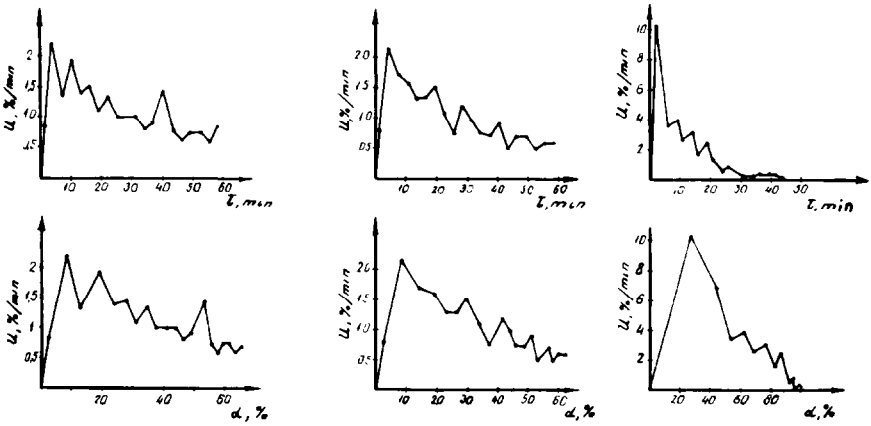

Fig. 7. Kinetic curves (by gas analysis) for ZnS lamellae oxidized at 1073 K, where τ is the time, α is the degree of conversion and u is the rate of the process.

cracks of a partially oxidized sample (Fig. 8) using a scanning electron microscope. The growth of these peculiar crystal formations takes place in free space in a gas medium. Most probably some sublimation and dissociation of ZnS take place with consecutive oxidation of the metal to ZnO and oxidation of the existing oxide cores. These processes are of real importance at temperatures higher than 1223 K.

Formation of a laminar and very porous oxide product (Fig. 9) is also found in the oxidation of natural samples of ZnS.

The porous texture of the product, established by us, entirely explains the kinetic regime, stated earlier [15,30], of ZnS oxidation in a fluid bed.

On isothermal, high-temperature pyrite oxidation Jorgensen and Moyle [42] also found a multi-layer structure of the partially oxidized sulphide

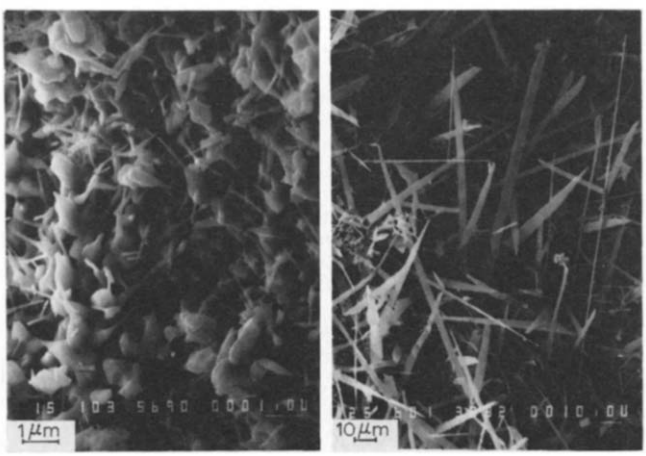

Fig. 8. Inner surface of a partially oxidized sample of ZnS, SEM.

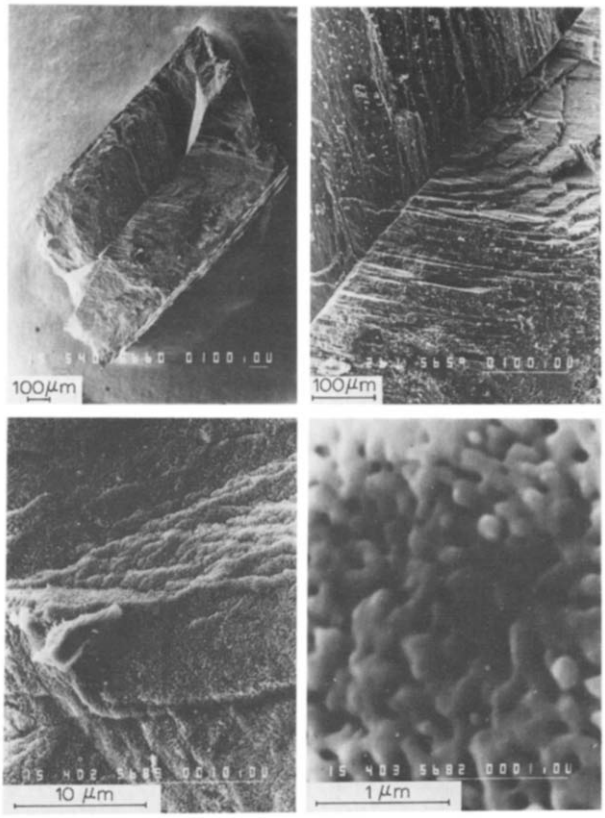

Fig. 9. Electron microscope picture of sphalerite lamellae, oxidized at 1073 K for 1 h.

grains. Our investigations with a scanning electron microscope also show in this case, that porosity of the oxide product is determined not only by interlayer cracks, as those authors suggest, but also by the substantial porosity of each individual oxide layer.

The detailed microscope and microdrill investigations of enlarged calcined particles from an industrial furnace for roasting zinc concentrates in a fluid bed show that the process of oxidation proceeds analogously to that in separate ZnS particles.

The diameters of the calcined granules are as large as 1×10^{-2} m. Their cross sections consist of two concentric zones: an outer, unoxidized one (an agglomerate mainly of sphalerite particles of 20–50 μm); and an inner one (oxide porous mass, which is abundant in laminar pseudomorphoses on the sphalerite particles). Iron is an independent phase (hematite (Fe_2O_3)). Included uniformly in the oxide product, it gives a red-brown colour.

Individual incompletely oxidized sphalerite particles of multi-layer ZnO coating (Fig. 10) establish around the inner boundary of the oxide zone. The content and distribution of the separate phases are determined with a

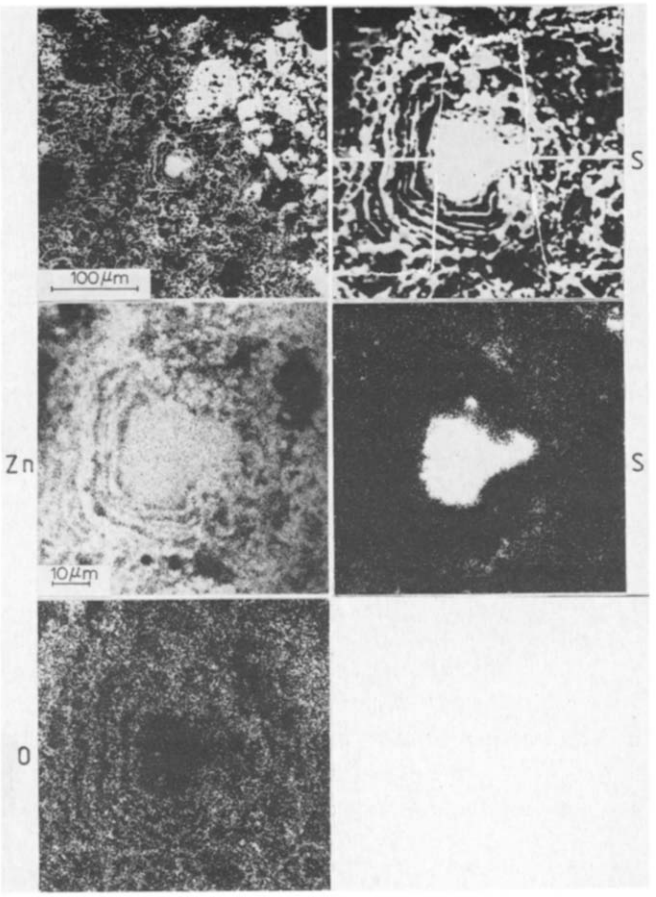

Fig. 10. Characteristics of an oxide coating of an enlarged particle from a fluid bed furnace on roasting zinc charges (1223 K) and results from the X-ray microanalysis for Zn, S and O.

microanalyser through area and profile scanning of the characteristic rays of the basic elements. Compared to synthetic sulphide (Figs. 3 and 5) the oxide layers of the concentrate are substantially narrower (2–5 μm).

The high porosity and laminar character of the oxide product indicate a decreased diffusion resistivity and oxidation in a kinetic regime up to high temperatures (for instance 1250 K) and to a high degree of transformation (Table 1).

CONCLUSION

The following mechanism of ZnS oxidation is suggested on the grounds of the theory of heterogeneous "solid–gas" reactions, the reference data and

the results, obtained by us from the complex investigations carried out, using different modern methods.

Oxidation of ZnS surface (first stage, first layer)

The process includes the following steps:

(1) Supply of gaseous reagent from the air stream to the sulphide surface;

(2) chemisorption of oxygen;

(3) chemical interaction: oxidation of ZnS with ZnO and SO_2 production, a topochemical process [43];

(4) ZnO crystal growth;

(5) desorption of the gaseous product (SO_2) from the particles in a gas stream;

(6) separation of the surface ZnO layer.

Proceedings of the process in the depth of the particles (from the 2nd to the i-*th layer)*

The process includes the following steps:

(1) supply of gaseous reagent from the air stream through the boundary gas layer towards the oxidized surface of the particle:

(2) air diffusion through the pores, channels and cracks of the multilayer oxide product towards the "moving" surface of reaction;

(3) chemisorption of oxygen on the surface of the unreacted sulphide core;

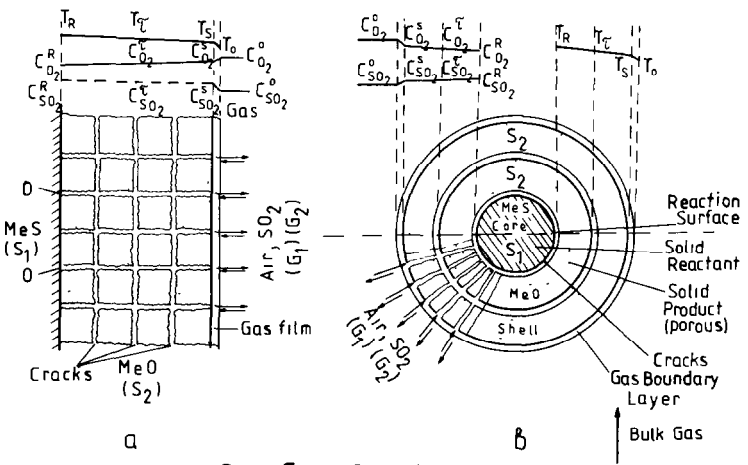

$$S_1 + G_1 \longrightarrow S_2 + G_2$$

$$MeS + O_2 \longrightarrow MeO + SO_2 \quad (\Delta H < 0)$$

Fig. 11. Structural models for oxidation of: lamellae (a), spherical ZnS particle (b).

(4) chemical interaction: ZnS oxidation with ZnO and SO_2 production, a topochemical process;

(5) ZnO crystal growth;

(6) SO_2 desorption from the reaction surface towards the pores, channels and cracks of the oxide layer;

(7) gaseous product diffusion from the reaction surface.

Structural model for ZnS oxidation

The following structural models of lamellar and spherical ZnS oxidation (Fig. 11a and b) may be suggested on the grounds of the results of our investigations of the mechanism and kinetics of ZnS oxidation and the literature data [10,18,44,45,etc.]. Figure 12 shows a comparison of the models offered in different publications.

The model suggested by us reflects the porous and laminar character of the solid product obtained and explains more clearly the results from the kinetic investigations and the behaviour of sulphide particles in the process. At the same time, this structural model allows the suggestion of a suitable model, of accuracy adequate for practice, for mathematical modelling of the processes of oxidation in a fluid bed furnace. This would allow automatic control of sophisticated processes taking part in a roasting reactor [46].

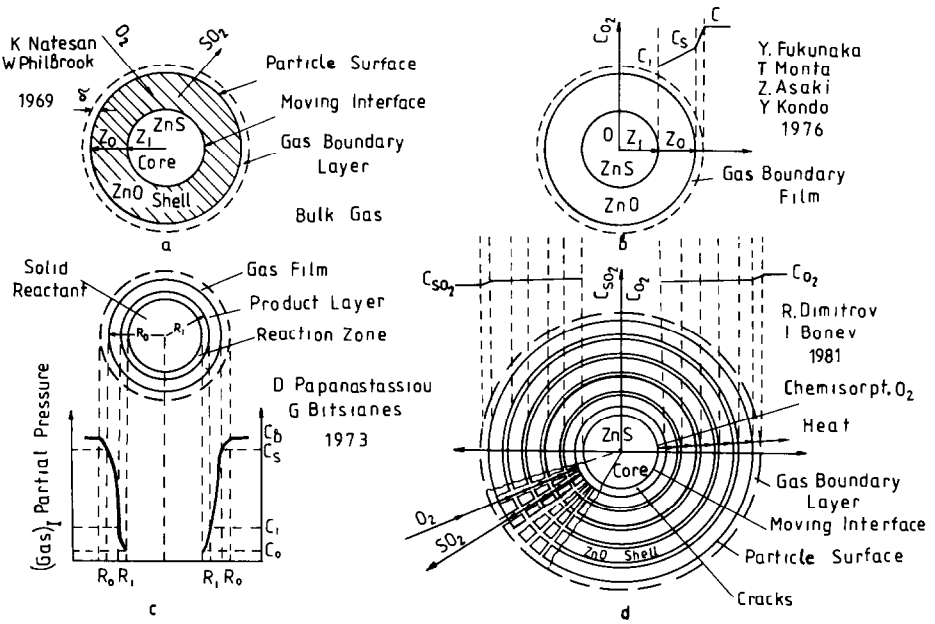

Fig. 12. Structural models for spherical particle oxidation from different authors.

REFERENCES

1 B.I. Scachkov, Thesis, Baykov Institute for Metallurgy, Moscow, 1953.
2 J. Ong, M. Wadsworth and W. Fassel, J. Met., 8 (1956) 257–263.
3 K. Cannon and K. Denbigh, Chem. Eng. Sci., 6 (1957) 145–159.
4 K. Denbigh and G. Beveridge, Trans. Inst. Chem. Eng., 40 (1962) 23–34.
5 J. Gerlach and W. Stichel, Erzmetall, 8 (1964) 427–433.
6 I.A. Burovoy and V.A. Brjukvin, Coll. Works Gintsvetmet, Moscow, 21 (1964) 131–145.
7 M. Rao and K. Arbacham, Indian J. Technol., 3 (1965) 291–293.
8 R. Dimitrov and A. Paulin, Min. Metall. Q., 3–4 (1965) 5–27.
9 P. Thornhill and I. Pulgeon, J. Met., 9 (1967) 980–995.
10 K. Natesan and W. Philbrook, Trans. Metall. Soc. AIME, 245 (1969) 2243–2250.
11 R. Dimitrov and H. Vodenicharov, C.R. Acad. Bulg. Sci., 22 (1969) 727–730.
12 R. Dimitrov and H. Vodenicharov, C.R. Acad. Bulg. Sci., 22 (1969) 903–905.
13 K. Natesan and W. Philbrook, Metall. Trans., 1 (1970) 1353–1360.
14 W.-K. Lu, Trans. Metall. Soc. AIME, 227 (1963) 203–206.
15 R. Dimitrov and A. Vanjukov, Non-Ferrous Met., 3 (1970) 7–11 (in Russian).
16 E. Mendoza, R. Cunningham and J. Ronco, J. Catal., 17 (1970) 277–286.
17 R. Dimitrov, Natura (Plovdiv, Bulg.), 4 (1971) 85–88.
18 Y. Fukunaka, T. Monta, Z. Asaki and Y. Kondo, Metall. Trans., 78 (1976) 307–314.
19 T. Karwan and C. Malinovski, Thermochim. Acta, 17 (1976) 195–206.
20 T. Rosenqvist, Metall. Trans. B, 98 (1978) 337–351.
21 A. Yazawa, Metall. Trans. B, 108 (1979) 307–321.
22 H.Y. Sohn and R.P. Goel, Miner. Sci. Eng., 2 (1979) 137–153.
23 S. Shin, V. Kirkosjan and S. Korkija, Tsvetn. Metall., 1 (1981) 32–35.
24 I. Piskunov, T. Karwan, A. Orlov and C. Malinovski, Rudy Met. Niezelaz., 23 (1981) 527–533.
25 L.A. Danilin, Izv. Vyssh. Uchebn. Zaved., Tsvetn. Metall., 2 (1982) 110–115.
26 R. Dimitrov and I. Bonev, Nove Vedechko technicke poznatky v hutnictve, Hutnictvo nezelaznych kovov-III sekcia, Kosice, CSSR, 1982, pp. 96–103.
27 R. Dimitrov, L. Avramov and P. Lesidrensky, Min. Metall. Q., 30 (1983) 269–273.
28 S. Kogahmetov, Z. Tumarbekov and M. Chokoev, Heavy Metal Sulphide Melts, Mir, Moscow, 1982, pp. 89–96.
29 R. Dimitrov, I. Dokuzov, A. Heckimova and T. Genevska, Yearb. Inst. Non-Ferrous Metall. (Plovdiv), 20 (1982) 60–77.
30 R. Dimitrov and B. Boyanov, Min. Metall. Q., 30 (1983) 211–222.
31 R. Dimitrov and B. Boyanov, Thermochim. Acta, 64 (1983) 27–37.
32 R. Dimitrov, C.R. Acad. Bulg. Sci., 23 (1970) 1215–1218.
33 E.V. Margulis, Collected Research Works, Vnitsvetmet, Metallurgija, Moscow, 1968, Nos. 17, 5, 10, 10–21, 21–28.
34 G.S. Frentz, Oxidation of Metal Sulphides, Nauka, Moscow, 1964.
35 A. Vanjukov and V. Zaitsev, Theory of the Pyrometallurgical Processes, Metallurgija, Moscow, 1973.
36 R. Dimitrov, Min. Metall. Q., 30 (1983) 397–419.
37 K. Haufe, Reactions in Solid Bodies and on their Surfaces, Inostrannaja Literature, Moscow, 1963.
38 B. Delmon, Kinetics of the Heterogeneous Reactions, Mir, Moscow, 1972.
39 O. Levenspiel, Engineering Presentation of the Chemical Processes, Khimiya, Moscow, 1969.
40 F. Habashi, Fundamentals of Applied Metallurgy, I, Theoretical Fundamentals, Metallurgija, Moscow, 1975.
41 R. Dimitrov and B. Boyanov, Izv. Vyssh. Uchebn. Zaved., Tsvetn. Metall., 6 (1983) 28–34.

42 F.R.A. Jorgensen and F.I. Moyle, Metall. Trans. B, 12 (1981) 769–770.
43 A.Ja. Rozovskij, Kinetics of the Topochemical Reactions, Khimiya, Moscow, 1974.
44 D. Papanassion and G. Bitsianes, Metall. Trans., 4 (1973) 477–486.
45 C.Y. Wen and S.C. Wand, Ind. Eng. Chem., 62 (1970) 31–51.
46 R. Dimitrov, T. Dimov and T. Ivanov, Freiberg. Forschungsh. B, 251 (1985) 77.